

Hydrogels modified with QHREDGS peptide support cardiomyocyte survival *in vitro* and after sub-cutaneous implantation†‡

Fiona Rask,^{§a} Anton Mihic,^{§b} Lewis Reis,^c Susan M. Dallabrida,^d Nesreen S. Ismail,^d Krista Sider,^c Craig A. Simmons,^c Maria A. Rupnick,^e Richard D. Weisel,^b Ren-Ke Li^b and Milica Radisic^{*ac}

Received 11th May 2010, Accepted 5th July 2010

DOI: 10.1039/c0sm00362j

Myocardial cell injection and tissue engineering could provide novel treatment options for heart diseases; however both approaches are limited by the loss of the transplanted myogenic cells. We hypothesized that novel hydrogels could promote cardiomyocyte survival and remedy this critical limitation. The hydrogel described here is based on a photocrosslinked form of chitosan, Az-chitosan, which was covalently bound to the QHREDGS peptide to promote cell survival. The QHREDGS amino acid sequence is thought to be the integrin binding site in angiopoietin-1, a growth factor which has cardioprotective properties. Covalent immobilization was performed using 1-ethyl-3-(3-dimethylaminopropyl)carbodiimide chemistry. Elastic moduli of the Az-chitosan hydrogel were within the lower physiological range for the neonatal rat heart (1.9 ± 0.2 kPa for 10 mg/ml and 3.5 ± 0.6 kPa for 20 mg/ml). After 6 days of cultivation of neonatal rat heart cells encapsulated with the hydrogels, cell viability and elongation was significantly higher in the peptide modified groups compared to the Az-chitosan control. No significant differences were found in the ability of RGDS and QHREDGS hydrogels to support contractile function *in vitro*. After subcutaneous implantation of cardiomyocyte hydrogel-peptide constructs in Lewis rats for 7 days, both QHREDGS and RGDS similarly recruited endothelial cells. However, Az-chitosan-QHREDGS gel had a higher percentage of smooth muscle actin (SMA)-positive myofibroblasts. The QHREDGS peptide gel promoted cardiomyocyte elongation and assembly of contractile apparatus and reduced cardiomyocyte apoptosis significantly better than the RGDS peptide. The new Az-chitosan-QHREDGS hydrogel may markedly improve cardiac regeneration by cell therapy.

Introduction

Ischemic heart disease is the leading cause of death worldwide.¹ Myocardial infarction (MI) after occlusion of coronary arteries results in death of cardiomyocytes (CM) and formation of scar tissue that reduces cardiac function. Despite current interventional or surgical reperfusion strategies or pharmacological therapy, ventricular remodeling may progress, leading to irreversible heart failure. Cell transplantation is a promising therapeutic approach that has been evaluated in many clinical trials.

Several cell types have been investigated in these clinical trials; however, the benefits observed in preclinical studies have not been seen in patients.²⁻⁴ The modest improvements seen in humans are believed to be due to the paracrine release of cytokines by the transplanted cells, rather than physical integration of these cells with the endogenous cardiomyocytes.^{5,6}

Although cell therapies for cardiac regeneration show promise, they have been limited by modest cell survival and engraftment. The small number of remaining cells may be due to leakage of cells from the injection site following intramyocardial delivery and/or the limited survival of the cells in the hostile microenvironment of the infarcted heart.⁷ The application of tissue engineering techniques to cell transplantation may enhance cell retention and survival.⁸ *In vivo* engineered tissue, enhanced by injectable biomaterials, provides cells with a temporary matrix for adhesion to improve survival and physically retain cells at the injection site. In addition, pharmacological agents and growth factors can be incorporated into the biomaterials to improve angiogenesis and augment the paracrine benefits provided by the engrafted cells.⁹ Several *in vivo* studies investigating injectable biomaterial systems have provided encouraging results in small animal models of MI.¹⁰⁻¹⁴ Thus, cardiomyocytes cultured on an injectable hydrogel matrix could be used to repair injured myocardium.

An ideal hydrogel to enhance cardiomyocyte engraftment should be (i) biocompatible, (ii) biodegradable, (iii) injectable (so that it can be applied with a syringe in a minimally invasive

^aDepartment of Chemical Engineering and Applied Chemistry, University of Toronto, Toronto, ON, Canada. E-mail: m.radisic@utoronto.ca; Fax: +416-978-4317; Tel: +416-946-5295

^bDivision of Cardiovascular Surgery, Toronto General Research Institute, University Health Network, Toronto, ON, Canada

^cInstitute of Biomaterials and Biomedical Engineering, University of Toronto, Toronto, ON, Canada

^dHarvard Medical School, Center for Vascular Biology Research, Beth Israel Deaconess Medical Center, Boston, MA, USA

^eHarvard Medical School, Brigham and Women's Hospital, Cardiovascular Division, Boston, MA, USA

† Electronic supplementary information (ESI) available: Double staining for TUNEL and cardiac troponin I indicates less apoptotic nuclei in QHREDGS compared to the RGDS modified Az-chitosan. See DOI: 10.1039/c0sm00362j

‡ This paper is part of a joint *Soft Matter* and *Journal of Materials Chemistry* themed issue on Tissue Engineering. Guest editors: Molly Stevens and Ali Khademhosseini.

§ Fiona Rask and Anton Mihic have equally contributed to this paper.

manner) and (iv) mechanically stable enough to retain cells at the injection site. The stiffness of the biomaterial should match that of the native tissue. For cardiomyocyte therapy, the biomaterial should enhance the survival of the applied myogenic cells and the surrounding surviving cardiomyocytes. Following a coronary occlusion, cardiomyocyte loss is progressive and persists for up to 60 days after an MI. Up to 35% of cardiomyocytes at the border of an infarct become apoptotic during this time.⁷

Chitosan, a linear polysaccharide, is a natural hydrogel derived through the deacetylation of chitin, and is an ideal biomaterial to augment cell transplantation. Chitosan is naturally biocompatible, angiogenic, non-toxic and enhances wound healing.¹⁵ Medical implants coated with chitosan have shown minimal foreign body reactions confirming biocompatibility and anti-bacterial properties.¹⁶ The cationic nature of chitosan is also advantageous for applications in which adhesion to tissue is required, since tissue generally has a net negative charge.¹⁷ Chitosan is degradable *via* enzymatic hydrolysis by lysozyme. The rate of chitosan degradation can be altered by modifying the degree of deacetylation. Less deacetylation results in faster degradation.¹⁶

Several cell types encapsulated in chitosan-based materials had viability exceeding 80% for extended time periods.¹⁷ A photocrosslinkable form of chitosan, Az-chitosan, may be clinically useful since gelation occurs in less than 5 min following injection and exposure to UV light (365 nm), producing inert N₂ as the only byproduct. However, while Az-chitosan is biocompatible, the final cross-linked gel does not support cell attachment because the number of anchorage sites is reduced by crosslinking.¹⁸ Modification of Az-chitosan, with acryloyl-poly(ethylene glycol)-RGDS promotes *in vitro* cell attachment including neonatal rat cardiomyocytes.¹⁹ Angiopoietin-1 (ang 1) has been linked to cardiac regeneration, and interacts with select cardiomyocyte integrins to promote adhesion and cell survival. Ligand/integrin interactions regulate cardiomyocyte shape, adhesion, survival, differentiation, and contraction.^{20,21} The QHREDGS amino acid sequence was identified as the integrin binding site in ang 1 and a linear peptide of this sequence was sufficient to promote cardiomyocyte survival.²² This peptide may also facilitate cardiomyocytes to connect and promote syncytium formation. We previously demonstrated that the QHREDGS peptide prevented caspase 3 activation in cardiomyocytes cultivated as a monolayer on thin layers of peptide-linked hydrogels.²³ However, the *in vivo* effectiveness of this peptide has not been explored. Therefore, we show here that QHREDGS peptide-linked to our novel biomaterial promotes cardiomyocyte attachment and viability both in *in vitro* engineered constructs and after *in vivo* implantation.

Experimental section

Synthesis of Az-chitosan

Az-chitosan was synthesized according to a procedure previously described with modification. Chitosan (75% to 90% deacetylated chitin, Novamatrix, Norway) 400 mg was dissolved in 15 mL of distilled water.¹⁹ A mass of 140 mg of 1-ethyl-3-(3-dimethylaminopropyl)carbodiimide HCl (EDC, Thermo Scientific) was dissolved in 1 mL of distilled water and 80 mg of 4-azido-benzoic acid (ABA, TCI America) was dissolved in 1 mL of

DMSO. A 300 μ L aliquot of N,N,N',N'-tetramethylethylenediamine (TEMED, Sigma) was added to the ABA solution followed by the EDC solution. This final solution was added drop-wise to the dissolved chitosan solution. The pH of the solution was adjusted to 6 using 1 N HCl and then pH 5 after 10 min. The solution was covered to protect from light and left to react overnight.

The product was centrifuged at 11 500 \times g for 2 h the supernatant containing the Az-chitosan was collected, and the azido-benzoic acid rich precipitate discarded. The pH of the solution was increased to 9.5 using 1 N NaOH to precipitate the Az-chitosan. The tube was centrifuged at 15 200 \times g for 10 min and the supernatant containing impurities such as unreacted ABA was aspirated. The Az-chitosan pellet was dispersed in 80 mL of distilled water. The solution underwent the first purification, which involved adjusting the pH to 3 with 1 N HCl to dissolve the Az-chitosan, and then increasing pH to 9.5 to precipitate pure Az-chitosan. The tubes were centrifuged at 15 200 \times g for 10 min, the supernatant was aspirated and the pellet was dispersed in 80 mL of distilled water. This purification step was repeated until the absorbance of the supernatant was less than 0.01 at 270 nm to confirm that most of the unreacted ABA had been removed. After the final wash the pellet was resuspended in 40 mL of distilled water and the pH was adjusted to 5 using 1 N HCl. This solution was then lyophilized for 3 days and stored at -20 °C until use.

Conjugation of peptides to Az-chitosan

Peptide conjugation was performed using EDC chemistry as described previously.²⁴ Az-chitosan was dissolved at 20 mg/mL in 0.9% phosphate buffered saline (PBS) and the peptide QHREDGS was dissolved at 20 mg/mL in PBS, and RGDS (American peptide) was dissolved at 10 mg/mL in PBS. The reagents were combined with the powder form of EDC and S-NHS and PBS to achieve a final reaction solution of 2 mg/mL of Az-chitosan, 0.55 mg/mL EDC, 1.38 mg/mL S-NHS and 1.33 mg/mL of QHREDGS peptide; or 0.67 mg/mL of RGDS. The molar concentrations of RGDS and QHREDGS in the reaction solution and per mass of chitosan were similar (Table 3). The reaction proceeded for 6 h at room temperature and protected from light. This solution was dialyzed in a dialysis membrane (Spectra/Por MWCO 3500, Spectrum Labs) for 1.5 days and then filtered using a 0.2 μ m filter for sterilization. The solution was then lyophilized for 2 days.

Concentrations of covalently bound peptides in Az-chitosan

The covalent binding of peptides (QHREDGS or RGDS) to Az-chitosan was confirmed and quantified using fluorescently labeled forms of the peptides (FITC-C6-QHREDGS or FITC-C6-RGDS), with FITC conjugated to the N terminus of the peptides *via* N-aminohexanoic acid. A stock solution of 20 mg/mL was created by dissolving the FITC labeled peptides in PBS. This stock was then serially diluted to create 11 standards ranging from 0.05 μ g/mL to 50 μ g/mL. The standards were assessed by a fluorometer (Molecular Devices) at an excitation wavelength of 490 nm and an emission of 520 nm. Conjugation of fluorescently labeled peptides to Az-chitosan was performed as described above and the fluorescence of the peptide modified product was

determined using a fluorometer as described for the standard curve above. All of the samples were tested at a pH of 7 as the fluorescence is greatly affected by changes in pH.²⁵ The concentration of fluorescent peptide present in the reaction solution post-dialysis was determined by comparing the level of fluorescence against standards. The volume in the dialysis membrane increased to 7 mL after dialyzation and this volume was used to determine the mass of the conjugated peptide. The molecular weight cut off of the dialysis membrane was one-tenth the size of chitosan, so it was assumed that the membrane retained all of the chitosan. Therefore the mass of Az-chitosan was the amount initially used in the reaction (12 mg).

Scanning electron microscopy

Glass coverslips (12 mm diameter) were coated with 50 μ L of dissolved Az-chitosan (20 mg/mL), Az-chitosan-QHREDGS or Az-chitosan-RGDS (12 mg/mL) and cross-linking was achieved following 5 min exposure to UV light (UVP, 365 nm, 1 mW/cm² at 3" distance, 115 V, 60 Hz, 0.16 Amp). The samples were stored in PBS and analyzed by variable-pressure scanning electron microscopy (VP SEM) in an environmental chamber using a cold-stage adaptor (S-3400N, Hitachi). Surfaces were imaged with an accelerating voltage of 15 kV and representative images were acquired.

Mechanical testing

Az-chitosan was dissolved at 10 mg/mL and 20 mg/mL in 0.9% saline, and 100 μ L of the material was placed on 12 mm circular glass coverslips and crosslinked for 5 min as described above. The samples were stored submersed in PBS in 12 well plates. To determine the stiffness of the gels, micropipette aspiration (MA) was used.²⁶ Pipettes with an internal diameter of 0.21 mm were used to apply pressure locally in the centre of the gels. The pipette diameter was less than the thickness of the gel, ensuring that only the stiffness of the gels and not the underlying glass was measured.²⁶ Pipette placement was controlled by a micromanipulator. Pressure was applied using a 20 mL air filled syringe attached to a linear actuator, which applied 0.01–0.05 cm steps (~1–3 kPa) at 400 Hz controlled by LabView. The maximum applied pressure was 6–14 kPa. Images were captured immediately after each step using PSRemote through a Navitar 12 \times zoom lens connected to a digital camera. Three to four measurements were made per gel concentration. Aspiration lengths for each step were measured and normalized to the pipette diameter. The initial elastic modulus (representative of the physiological range²⁷) was estimated using an analytical half-space model that is commonly applied to analyze MA data.²⁸

Degradation studies

A volume of 100 μ L of 10 mg/mL Az-chitosan, QHREDGS modified Az-chitosan, and RGDS modified Az-chitosan, were placed on coverslips and crosslinked with UV light for 5 min as described above. The coverslip with the material was placed in a Petri dish and the mass of this entire system determined. Cardiomyocyte culture media containing 10% fetal bovine serum (FBS), was added to the Petri dish and the samples were stored in a 37 °C incubator to simulate the conditions used for cell culture

and *in vivo* studies. To assess the weight of the material at different time points, the media was aspirated and the mass of the sample in the Petri dish measured.

Isolation of neonatal rat cardiomyocytes

All animal experimental procedures were approved by the Animal Care Committee of the Toronto General Research Institute and the University of Toronto Committee on Animal Care, according to the Guide for the Care and Use of Laboratory Animals. Neonatal (1 to 2 day-old) Sprague-Dawley (*in vitro* studies) or Lewis rats (*in vivo* studies) were euthanized, hearts were removed and primary cardiomyocytes isolated as described.^{29,30} The cardiomyocyte culture medium consisted of Dulbecco's Modified Eagle medium with 4.5 g/L glucose, 4 mM L-glutamine, 10% FBS and 100 U/mL penicillin/streptomycin. Cells were maintained in a humidified 5% CO₂ incubator at 37 °C.

Monolayer studies

Hydrogen peroxide treatment

Rat neonatal cardiomyocytes were incubated for 1.5 h with 500 μ M QHREDGS, scrambled (scram) QHREDGS peptide (DGQESHR), or PBS control (PBS); 200 nM ang 1 or its matched buffer control [0.1% bovine serum albumin (BSA) in PBS] in the culture medium. The culture medium consisted of Dulbecco's Modified Eagle's Medium (DMEM) with 0.5% BSA and cytosine- β -D-arabinofuranoside (anti-proliferative). Reactive oxygen species were increased by addition of 100 μ M H₂O₂ for 10 min (37 °C, 5% CO₂) (N = 6/group). Cell viability was measured using a Trypan blue stain. Trypan blue dye is impermeable to viable cells, but enters dead/damaged cells with impaired membrane integrity, staining cells blue.

Doxorubicin induced apoptosis and caspase activation

Rat neonatal cardiomyocytes were given doxorubicin (Dox) to induce apoptosis and PBS or peptide QHREDGS (1 d), Western blotting was conducted as described³¹ and levels assessed *via* densitometric analysis (Scion Image software). Graphs show levels of inactive *versus* active caspase-3. Levels of inactive caspase-6 were normalized to GAPDH.

Adenosine triphosphate (ATP) assay

Rat neonatal cardiomyocytes were incubated with PBS (control), 500 μ M QHREDGS, scrambled QHREDGS peptide, GRGDSP peptide or 400 nM ang 1 or ang 2 in DMEM/0.5% BSA/cytosine- β -D-arabinofuranoside (37 °C, 5% CO₂, 1 d). ATP levels were quantified using the CellTiter-Glo Luminescent Assay (Promega) as per manufacturer's instructions (N = 6/group). Luminescence was measured using a Wallac 1420 microplate reader.

Cardiomyocyte encapsulation system

The lyophilized form of the peptide-modified Az-chitosan (Az-chitosan-QHREDGS or Az-chitosan-RGDS) was dissolved in sterile 0.9% NaCl at 12 mg/mL. Cardiomyocytes (2.5 \times 10⁶) were suspended in 15 μ L 30% FBS-containing culture medium for 15 min on ice. These cells were further suspended in 35 μ L of the

hydrogel. This mixture was placed on a 12 mm diameter glass coverslip, which was placed on a UV lamp (UVP, 365 nm, 1 mW/cm² at 3'' distance, 115 V, 60 Hz, 0.16 Amp) and exposed to UV light for 5 min. The samples were then transferred to a 12 well plate and supplemented with 2 mL of warm cardiomyocyte culture media.

Live/dead staining

Live/dead staining was performed using 5-carboxyfluorescein diacetate acetoxyethyl ester, which stains live cells green, and propidium iodide, which stains dead cells red according to the manufacturer's instruction (Invitrogen). Three sets of surfaces were analyzed for each sample type.

Functional testing

The electrical function of *in vitro* samples of neonatal cardiomyocytes encapsulated in chitosan hydrogels for 6 d was established by measuring excitation threshold (ET), the minimum voltage required to pace the encapsulated cells simultaneously, and maximum capture rate (MCR) as we described.²⁹ The MCR is the maximum stimulation rate at which the encapsulated cardiomyocytes can be induced to beat simultaneously. The encapsulated samples were placed between a pair of carbon electrodes immersed in warm Tyrode's solution (Sigma, pH 7.4). The ET was measured by stimulating the samples with square pulses of 2 ms width at a frequency of 1 Hz and increasing the output voltage of the stimulator until ~90% of the cells in the field-of-view were beating synchronously with the stimulator output. The MCR was measured by setting the output at 15 V, and increasing the frequency until most of the cells in the sample were no longer synchronously beating with the driving signal. All measurements were taken using bright field microscopy. The samples were placed in an environmental chamber at 37 °C for the measurements (N = 3/group).

Sample preparation for *in vivo* implantation

Cardiac constructs were made by encapsulation of neonatal Lewis rat cardiomyocytes in Az-chitosan-QHREDGS or Az-chitosan-RGDS. A total of 2×10^6 cardiomyocytes were resuspended in 15 μ L of ice cold cardiomyocytes medium with 30% FBS for at least 10 min. These cells were then encapsulated in 100 μ L of the hydrogel in transwell plates and constructs (2 mm thick and 6 mm in diameter) were produced. A total of 8 samples were made for each type of hydrogel, and 4 from each group were implanted, while the other 4 were retained as *in vitro* controls. Samples were cultured at 37 °C for 5 d before they were implanted *in vivo*.

Subcutaneous implantation and histological assessment

Cardiac constructs described above were inserted subcutaneously into the abdomen of Lewis rats. Four samples were implanted for each type of hydrogel. Animals were observed for 7 d and then implanted tissues recovered. Histological sections of 4–5 μ m were prepared from samples frozen in O.C.T. compound and stained for hematoxylin and eosin (H&E), smooth muscle actin (SMA) and Factor VIII as described.³² Quantification of

total SMA and Factor VIII was performed using ImageScope v10 (Aperio Technologies) and mean intensities were averaged for six fields for each sample and normalized to total area. Immunofluorescence staining was performed on frozen sections for cardiac sarcomeric α -actinin, and troponin I as described.³³ Apoptosis was assessed using a TUNEL assay (Roche Applied Science) following the manufacturer's standard protocol.

Statistical analyses

All data are expressed as mean \pm S.E.M. and "n" is the number of experiments per group. Unpaired student's t tests or one-way ANOVAs were used to compare among experimental groups. Data was analyzed using Prism 4.0c (Graphpad Software, Inc.) and a $p < 0.05$ was considered statistically significant.

Results and discussion

Effect of soluble QHREDGS peptide on neonatal cardiomyocytes in monolayer culture

Superoxide burst is one of the major causes of cardiomyocyte death upon reperfusion. We therefore tested the ability of ang 1 and QHREDGS peptide to prevent cell death in cardiomyocytes treated with H₂O₂ *in vitro*. Our data show that with H₂O₂, cardiomyocyte viability declines to under 50% (Fig. 1A). In contrast, we found that ang 1 and peptide QHREDGS maintain cardiomyocyte viability after exposure to H₂O₂. Therefore, ang 1 and QHREDGS peptide effectively protect neonatal rat cardiomyocytes against cell death and injury induced *in vitro*.

Doxorubicin (Dox) is another potent agent which induces apoptosis in cardiomyocytes. We evaluated the ability of QHREDGS peptide to protect cardiomyocytes against Dox-induced apoptosis by evaluating activation of caspase-3 and -6. These caspases are considered end-stage executioner caspases; however increases in their activity may not always lead to cell death. For example, a lesser amount of caspase-3 activation will not commit cells to die, but rather can cause proteolysis and degradation of cardiomyocyte contractile proteins, and thus, substantially impair myocyte contractility, which can depress cardiac function. Our data clearly indicate that activation of caspases-3 and -6 were blocked by doses of QHREDGS peptide as low as 5 μ M (Fig. 1B,C). Whereas peptide free controls given doxorubicin (PBS + Dox) exhibited a significant decrease in the presence of the inactive forms of caspase-3 and 6, the groups treated with QHREDGS peptide maintained the levels of inactive caspases at comparable amounts to the doxorubicin-free controls (PBS) (Fig. 1B,C).

ATP is the leading source of energy and metabolism in cardiomyocytes, thus ATP levels are critically important for cardiac cell function. In serum-starved conditions, both QHREDGS peptide and ang 1 substantially increased cardiac myocyte ATP levels, whereas scrambled QHREDGS, RGD-based peptides, and ang 2 had no such effect (Fig. 1D). Improving myocyte energetics in the adverse condition of serum-deprivation would be beneficial to attenuating the progression of cardiac injury, as occurs in cardiovascular disease.

Overall, these monolayer studies demonstrate that the QHREDGS peptide applied in the soluble form in the culture media protects cardiomyocytes against cell death inducing agents

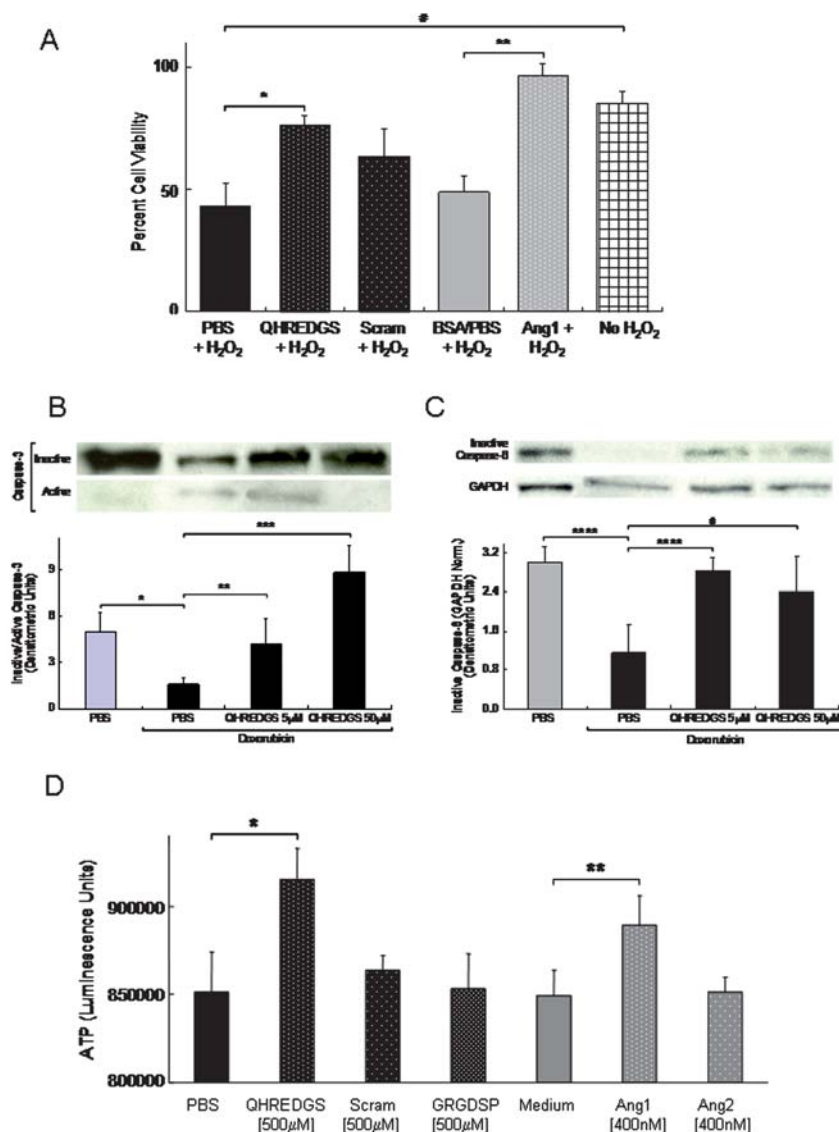


Fig. 1 QHREDGS exhibits cardioprotective properties on cardiomyocytes in monolayer culture. (A) QHREDGS peptide and ang 1 increase cardiomyocyte viability under conditions of oxidative stress. * $p = 0.009$, ** $p = 0.003$, # $p = 0.002$ ($N = 6$ /group). (B,C) QHREDGS peptide blocks doxorubicin-induced caspase-3 and -6 activation. Rat neonatal cardiomyocytes were given doxorubicin (Dox) to induce apoptosis and PBS or peptide QHREDGS (1 d). Graphs show (B) levels of inactive *versus* active caspase-3 and (C) levels of inactive caspase-6 normalized to GAPDH. Baseline values for both caspases in the absence of doxorubicin are shown as gray bars. Ang 1-derived peptide QHREDGS significantly blocked activation of (B) caspase-3 compared to controls (p values * $=0.02$, ** $=0.04$ and *** $=0.0008$) and (C) caspase-6 compared to the controls (p values **** $=0.01$ and # $=0.05$). (D) QHREDGS peptide and ang 1 increase ATP levels in serum-starved cardiomyocytes. Both QHREDGS peptide (* $p = 0.008$) and ang 1 (** $p = 0.03$) increased cardiomyocyte ATP levels, whereas scrambled QHREDGS, RGD-based peptides, and ang 2 had no such effect ($N = 6$ /group).

and maintains cardiomyocyte energetics. Thus, we next focused on determining if the covalently immobilized peptide in the hydrogel backbone could similarly preserve cardiomyocyte viability both *in vitro* and *in vivo*.

Properties of the peptide modified hydrogels

The elastic moduli of the base material, Az-chitosan, were assessed by micropipette aspiration at two concentrations (10 mg/mL and 20 mg/mL). For comparison, micropipette aspiration was also performed using neonatal and adult rat hearts. The modulus of the 20 mg/mL Az-chitosan hydrogel was

significantly greater than that of the 10 mg/mL Az-chitosan hydrogel (Table 1) as expected. The moduli of the 20 mg/mL Az-chitosan samples approached that of the neonatal rat heart tissue; however, they were not as stiff as adult rat hearts (Table 1). Cardiomyocytes themselves are particularly sensitive to the physical characteristics of their surrounding environment. Scaffold stiffness has been demonstrated to affect contractility of cardiomyocytes.^{34,35} Cardiomyocytes cultured on stiff fibrotic-like substrates lose their spontaneous contractile activity quickly, whereas cells grown on elastic substrates mimicking cardiac tissue preserve contractility for longer time periods.³⁶

Table 1 Elastic moduli of Az-chitosan samples and native hearts of Sprague-Dawley rats^a

Sample type	Elastic moduli (kPa)
Az-chitosan (10 mg/mL)	1.9 ± 0.2 (1.7–2.0)
Az-chitosan (20 mg/mL)	3.5 ± 0.6 (2.9–4.2) ^c
Neonatal heart of Sprague-Dawley rat ^b	4–11.4
Adult heart of Sprague-Dawley rat ^b	11.9–46.2

^a N = 3–4 measurements were made per group. ^b As reported previously.³⁵ ^c Significantly higher than the 10 mg/mL gel (p < 0.01).

Azidobenzoic acid modification of chitosan, with an identical conjugation protocol, was confirmed in our previous studies by ¹H NMR. ²³ Conjugation efficiencies of QHREDGS and the RGDS peptides to Az-chitosan were quantified using fluorescently tagged peptides. There were no significant differences in conjugation efficiencies between the two peptides. On average ~50% of the peptide added to the reaction solution was conjugated to Az-chitosan, specifically 57.6 ± 5.8% for QHREDGS and 46.0 ± 7.1% for RGDS (Table 2). Therefore, the molar concentration of the two different peptides per gram of Az-chitosan was comparable (Table 3).

Scanning electron microscopy of crosslinked chitosan hydrogels evaluated the three-dimensional surface structure of the hydrogels. Use of a cold-stage adaptor and VP SEM assisted in the preservation of surface structure and limited sublimation of frozen water. Representative images of Az-chitosan, Az-chitosan-QHREDGS, and Az-chitosan-RGDS coated glass coverslips qualitatively demonstrate the porous nature of the hydrogels (Fig. 2B–D). In contrast, the control glass substrate exhibited a smooth surface (Fig. 2A). Hydrogel porosity is desirable for encapsulated cells and permits sufficient nutrient and oxygen diffusion throughout the material. The Az-chitosan hydrogel possessed the highest degree of porosity, while the Az-chitosan-QHREDGS and Az-chitosan-RGDS hydrogels were slightly less porous. This is likely due to crosslinking, as the peptide-modified hydrogels may have additional EDC-induced crosslinking between peptides. However, the largest pores in peptide-modified hydrogels were 70–80 μm in diameter, thus potentially allowing cell penetration and elongation. Fiber-like structures, 3–4 μm, in diameter were also observed in all samples (Fig. 2B–D).

In humans and animals, chitosan degrades by hydrolytic action of lysozyme, an enzyme present in plasma (9–17 μg/ml³⁷). Biodegradation products are lower molecular weight chitosans, chito-oligomers, and monomers (N-acetyl-D-glucosamine, D-glucosamine). The presence of serum in culture media, prompts chitosan degradation, but at a lower rate than *in vivo*. Thus, we assessed hydrogel degradation in serum containing culture medium at 37 °C. Over 11 days *in vitro*, there were no significant differences in percent degradation between the groups, indicating that peptide modification did not significantly affect this property (Az-chitosan: 15 ± 37%, QHREDGS modified Az-chitosan: 19 ± 10% and RGDS modified Az-chitosan: 17 ± 7%, N = 3 per group).

Cultivation of cardiomyocytes encapsulated in chitosan hydrogels

Cardiomyocytes were encapsulated in Az-chitosan, Az-chitosan-RGDS and Az-chitosan-QHREDGS hydrogels and crosslinked

Table 2 Quantification of conjugation efficiency for covalent binding of peptides to Az-chitosan. Measured values reported as mean ± SD. No significant difference between conjugation efficiency of the two peptides, p = 0.21

Peptide	Mass in reaction solution (mg)	Concentration in reaction solution (mg/mL)	Theoretical concentration post dialysis (mg/mL)	True concentration post dialysis (mg/mL)	Mass peptide/mass Az-Chitosan (mg/mg)	Conjugation efficiency
FITC-C6-QHREDGS	4	1.33	1.14	0.66 ± 0.07	0.38 ± 0.04	57.6 ± 5.8%
FITC-C6-RGDS	2	0.67	0.57	0.26 ± 0.04	0.15 ± 0.02	46.0 ± 7.1%

Table 3 Estimated molar concentrations of peptides conjugated to Az-chitosan based on conjugation efficiencies in Table 2

Peptide	Mass in reaction solution (mg)	Molecular weight (g/mol)	Concentration in reaction solution ($\mu\text{mol/mL}$)	Number of moles of peptide per mass of chitosan ($\mu\text{mol peptide/g Az-chitosan}$)
QHREDGS	4	827.81	1.61	0.54
RGDS	2	433.42	1.54	0.41

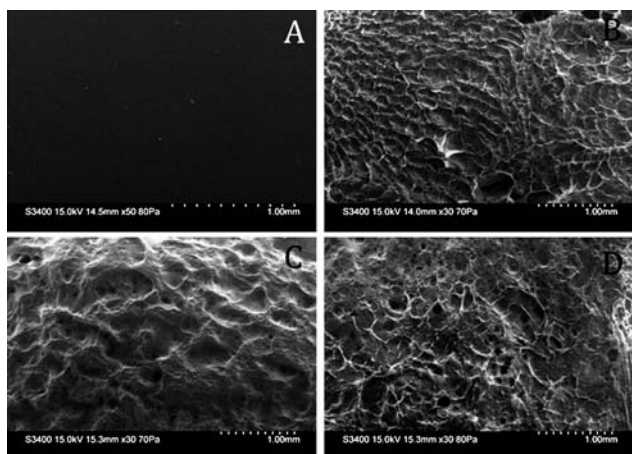


Fig. 2 Scanning electron microscopy of hydrogel surface porosity. (A) Uncoated glass coverslip and hydrogel-coated coverslips (B) Az-chitosan; (C) Az-chitosan-QHREDGS and (D) Az-chitosan-RGDS. Hydrogels were crosslinked with UV light for 5 min and placed in PBS. Scale bars and chamber atmospheric pressures are indicated in each panel.

onto glass coverslips with UV light exposure. The hydrogel modified with the scrambled peptide control, DGQESHR, was not pursued in our current studies, since our previous studies show that Az-chitosan-DGQESHR does not support myocyte viability longer than 3 days in monolayer culture or prevent taxol-induced apoptosis.²³ Live/dead cell staining was performed after 6 days of static cultivation to determine cell viability (Fig. 3). Peptide-modified hydrogels contained considerably more encapsulated live cells than the Az-chitosan control. In fact, no cells were observed visibly contracting in the Az-chitosan control group, which corresponded with the observed lower cell viability. Neonatal rat cardiomyocytes in the Az-chitosan control group appeared rounded, whereas cells in peptide-conjugated hydrogels were elongated and rod-shaped. A similar trend was observed in the cultivated cardiomyocytes on hydrogel thin films, but to a lesser extent.²³



Fig. 3 Peptide-conjugated Az-chitosan enhances encapsulated cell viability *in vitro*. Six days after cultivation of encapsulated cells the viability of neonatal rat cardiomyocytes were assessed. Dead cells were stained red and live cells stained green. Representative images of (A) Az-chitosan; (B) Az-chitosan-QHREDGS and (C) Az-chitosan-RGDS are shown. Scale bar represents 100 μm .

The lack of cell-adhesive properties of Az-chitosan observed here and in our previous studies^{23,38} may be from a crosslinking-induced decrease in the free amine groups. Cells encapsulated in the peptide-modified hydrogels contracted spontaneously with large areas of synchronization. The QHREDGS peptide resulted in the formation of a dense syncytium (Fig. 3B), which is critical for proper myocardial contractility, whereas only islands of connected cells were observed in the RGDS modified hydrogel (Fig. 3C). These observations confirm the ability of these peptides to promote the attachment and viability of the neonatal rat cardiomyocytes in the peptide Az-chitosan hydrogel system. These findings also confirm that the peptide-modified hydrogels possessed sufficient porosity to support cell survival in an encapsulated system over a prolonged time in culture. The small amount of hydrogel degradation during culture likely facilitated the cell linkage and syncytium formation.

During cultivation, regions of spontaneously contracting cardiomyocytes were observed in the peptide modified groups. Electrical field stimulation was employed at the end of the cultivation period to determine the functional capacity of the encapsulated neonatal rat cardiomyocytes. Similar to native heart tissue, the response of isolated cardiomyocytes to electrical stimulation is indicative of cell viability and functional capability.³⁹ Cardiomyocyte contraction could not be induced following encapsulation in Az-chitosan controls. The entire constructs containing myocytes plus Az-chitosan-QHREDGS or Az-chitosan-RGDS hydrogel beat synchronously (Table 4). There were no significant differences in excitation threshold (ET), minimum voltage required to pace the encapsulated cells simultaneously, or the maximum capture rate (MCR) between the cells encapsulated in the QHREDGS *versus* RGDS hydrogel (Table 4). Thus, the type of peptide did not significantly affect contractile properties in this hydrogel system.

The recordings obtained from our electrical stimulation experiments show that encapsulated neonatal cardiomyocytes can respond to external electrical stimulation. However, both hydrogels had a significantly higher ET than the neonatal rat

Table 4 Electrical excitability of the encapsulated heart cells after six days of cultivation. The first value of the ET corresponds to the external voltage applied at which contractions of cardiomyocytes first start to occur. The second value of ET corresponds to the complete construct synchronization^a

	ET (V/cm)	MCR (pps)
Neonatal rat heart	3.2 ± 1.5	5.7 ± 1.1
Cells encapsulated in Az-chitosan-QHREDGS	7.0 ± 0.4; 9.2 ± 0.6	4.3 ± 0.1
Cells encapsulated in Az-chitosan-RGDS	7.5 ± 0.7; 9.3 ± 0.5	4.1 ± 0.5

^a ET–excitation threshold; V–volts; MCR–maximum capture rate; pps–pulses per second.

heart, indicating that the cultivation system could be improved. Some of the improvements may include increasing the cell seeding density⁴⁰ or applying electrical field stimulation during cultivation.²⁹ Additionally, it may suggest that the coupling of encapsulated neonatal cardiomyocytes does not sufficiently mimic that of native heart tissue. The MCR was slightly reduced in the peptide-conjugated hydrogels compared to native heart. Following the isolation of neonatal cardiomyocytes and their hydrogel encapsulation, cell viability ranged from 50–70%, and therefore dead cells were also encapsulated and trapped in the system. Dead cells do not efficiently propagate electrical signals, thereby adversely affecting the functional parameters measured

during this study. In future studies, removal of dead cells by *e.g.* density gradient centrifugation may enhance the functional capability of the *in vitro* construct.

Subcutaneous implantation and *in vivo* assessment of cardiomyocyte/hydrogel constructs

To assess the *in vivo* response, cardiomyocyte/hydrogel (Az-chitosan-RGDS or Az-chitosan-QHREDGS) constructs were implanted after 5 days of *in vitro* cultivation. The need to maintain the implant shape and the matrix connections consistent for this initial assessment, motivated our decision to implant the constructs, rather than to directly inject cardiomyocyte/hydrogel mixture subcutaneously. Immunocompetent syngeneic Lewis rats were selected as cell donors and implant recipients to enable the full evaluation of the *in vivo* host response. The animals were healthy upon completion of the study (7 days post-implantation), and showed no external signs of inflammation. Upon retrieval of the constructs, no spontaneous contractions of the nodules were observed.

For *in vivo* studies, we assessed for the presence of cells that are involved in angiogenesis [endothelial cells (Factor VIII positive)], and wound healing [myofibroblasts/smooth muscle cells (SMA positive)] (Fig. 4) and cardiomyocytes (troponin I positive and sarcomeric α -actinin positive, Fig. 5) which are our target cell population. Further studies are necessary to characterize in detail

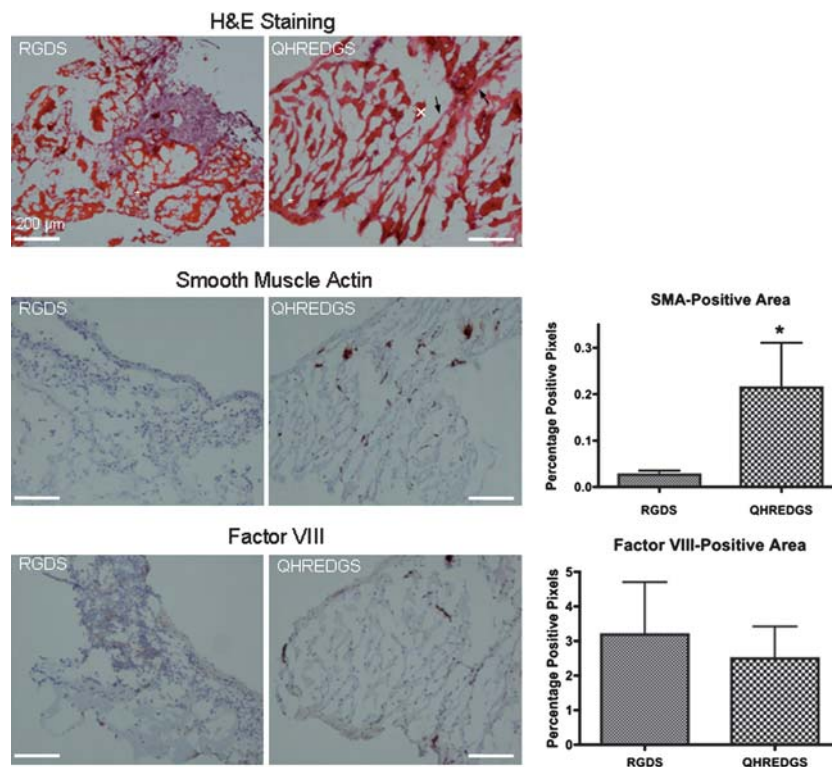


Fig. 4 RGDS and QHREDGS peptide modified chitosan hydrogels support similar endothelial cell recruitment into implants. Lewis rat neonatal cardiomyocytes were cultured for 5 days *in vitro* in peptide-modified chitosan hydrogel constructs (RGDS or QHREDGS). Constructs were subcutaneously implanted in Lewis rats for 7 days ($N = 4/\text{group}$) with no significant inflammatory response observed in either group upon completion of the study. H&E, smooth muscle actin and factor VIII staining show that both constructs retained their porous structure. Additionally, SMA staining was significantly stronger in the QHREDGS group ($p < 0.05$). The hydrogel pore walls can be seen in the slides (marked with x). Arrows indicate cells that are attaching to and spanning the pore walls.

the phenotypes and the relative amounts of the cells infiltrating the implanted nodule as well as to determine the effect of the RGDS and QHREDGS peptides on their survival and proliferation.

H&E staining qualitatively examined biomaterial degradation and tissue morphology, including the presence of encapsulated cells and additional autologous cell infiltration (Fig. 4A). Representative images show cell nuclei stained blue and cytoplasm stained light pink. The Az-chitosan hydrogels appear dark red in both images. Cells were located throughout the biomaterial in both groups (Fig. 4), mainly attached to the hydrogel pores and occasionally spanned the pores. On day 7, the hydrogels appeared to be largely intact, as evidenced by the presence of the large amount of dark red porous structures. The RGDS-conjugated Az-chitosan group appeared to have undergone a slightly greater degree of degradation due to cell infiltration as indicated by densely packed blue nuclei. The QHREDGS-conjugated hydrogel had less cell infiltration, suggesting little to no immune reaction against the implanted constructs.

The QHREDGS-conjugated hydrogels have a reduced inflammatory infiltrate similar to the full length parent protein, ang 1. Ang 1 has anti-inflammatory effects on the vasculature.⁴¹

In the skin of mice transgenically overexpressing VEGF, leukocyte adhesion to endothelial cells was decreased by coexpression of ang 1.⁴² This effect was mediated by inhibition of the expression of a number of inflammation-associated adhesion molecules including E-selectin, ICAM-1 and VCAM1.^{43,44} In addition, ang 1 has been shown to block TNF- α induced tissue factor expression in HUVECs.⁴⁵ The signaling mechanism for these anti-inflammatory actions remains to be identified, although inhibitor and dominant-negative experiments show that PI3K and Akt are required.^{43,45} Further evidence for the *in vivo* anti-inflammatory effects of ang 1 is provided by the decrease in leukocyte infiltration and fibrosis seen in cardiac allografts of rats overexpressing the ligand.⁴⁶ It is currently unknown, the extent to which peptide QHREDGS, mimics the anti-inflammatory properties of ang 1. Thus, our Az-chitosan-QHREDGS construct may serve as a tool to answer these questions in future *in vivo* studies.

Histological staining for SMA was also conducted to assess whether fibrosis occurred in the samples following implantation (Fig. 4). In these sections, SMA-positive tissue stained dark brown and cell nuclei stained blue. The SMA-positive staining was limited and diffuse in irregular patterns throughout the nodules. However, signs of significant fibrosis such as fibrotic encapsulation of the entire implant were absent. This staining pattern is consistent with the presence of myofibroblasts. Myofibroblasts play a key role in cardiac repair and stabilization following acute injury in the heart. In the weeks following wound healing, myofibroblasts undergo apoptosis and the resident fibroblasts continue to maintain normal cardiac remodeling.^{47,48} The presence of myofibroblasts in the Az-chitosan-QHREDGS hydrogel is consistent with this reparative process and provides an opportunity to characterize these complex cell interactions in engineered cardiac tissue.

Staining for Factor VIII was performed to identify blood vessel formation within the constructs (Fig. 4). Endothelial cells, which line blood vessels, are stained brown by Factor VIII. In 7 days, it was not sufficient time to identify distinct blood vessels within the nodules. We found similar extents of Factor VIII staining between the two peptide groups (Fig. 4), indicating that RGDS and QHREDGS peptides do not differ significantly in endothelial cell recruitment to the host.

To specifically identify and characterize cardiomyocytes within the hydrogel nodules, we carried out immunofluorescence staining using the cardiac-specific markers sarcomeric α -actinin and cardiac troponin I (Fig. 5). Proteins of interest were stained green and nuclei were stained blue. These cytosolic proteins exhibit distinct patterns and highlight the contractile apparatus of cardiomyocytes. Remarkably, the Az-chitosan QHREDGS-conjugated hydrogel possessed larger areas of cardiomyocytes compared to the RGDS-conjugated controls. Areas of healthy, elongated cardiomyocytes were observed, whereas the RGDS-conjugated hydrogel contained only round immature cardiomyocytes with limited cardiac-specific staining patterns. These findings indicate that the QHREDGS peptide was considerably better than the RGDS peptide in promoting the maturation of a differentiated cardiomyocyte phenotype in the setting of cell/hydrogel transplantation. As the hydrogels began to degrade, the encapsulated cell clusters not only maintained their contractile apparatus, but the clusters seemed to coalesce to

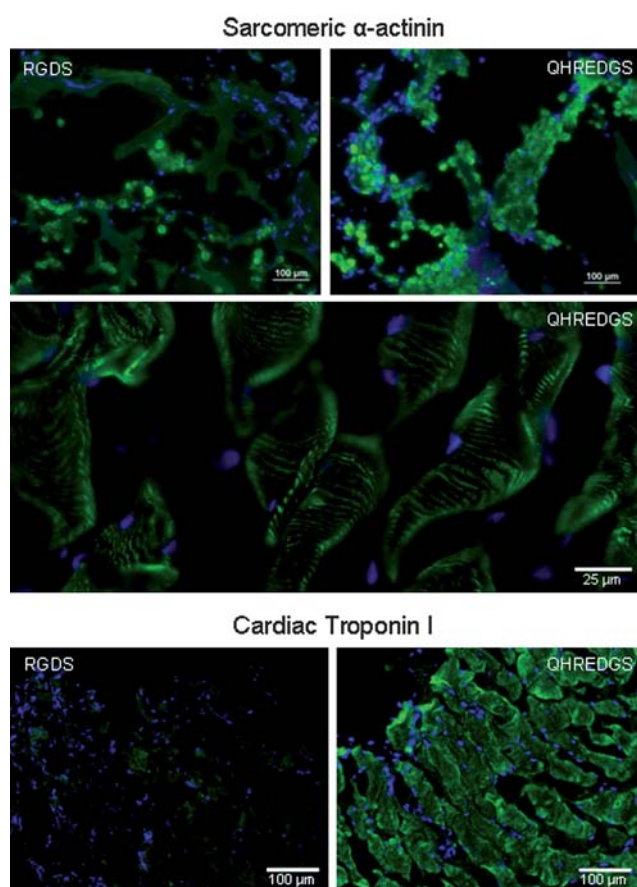


Fig. 5 QHREDGS peptide enhances cardiomyocyte phenotype *in vivo*. Immunofluorescence staining for cardiac markers, sarcomeric α -actinin and cardiac troponin I, after subcutaneous implantation. Subcutaneously implanted constructs ($N = 4$ /group) were removed after 7 days. Az-chitosan-QHREDGS enhanced cardiomyocyte elongation and maintained the phenotype compared to Az-chitosan-RGDS.

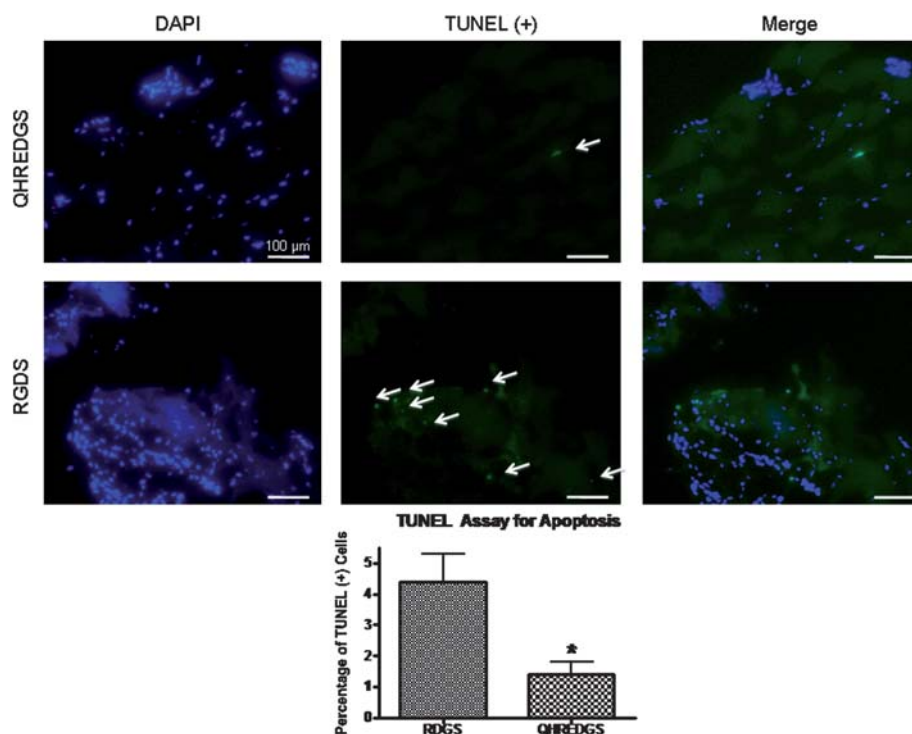


Fig. 6 QHREDGS reduces cell apoptosis *in vivo*. Subcutaneous implantation of cardiomyocytes in peptide modified chitosan hydrogels was examined for apoptosis using TUNEL staining ($N = 4/\text{group}$). TUNEL staining labeled apoptotic nuclei green, while nuclei were labeled blue with DAPI. The peptide QHREDGS reduced cell apoptosis during subcutaneous implantation of encapsulated cardiomyocytes.

form a syncytium. Cardiomyocytes were not beating at 7 days post-implantation. Future studies will determine how to maintain synchronous contraction of the encapsulated cells in order to use these constructs for cardiac reconstruction following a myocardial infarction.

Since the majority of cell death occurs early after construct implantation, while the implant is still not fully vascularized, we intentionally terminated the experiment at 7 days after implantation. TUNEL staining indicated significantly fewer apoptotic cells in the QHREDGS modified hydrogel compared to the RGDS peptide modified Az-chitosan (Fig. 6). In addition, double staining for cardiac troponin I and TUNEL indicated fewer apoptotic cardiomyocytes in the QHREDGS modified hydrogel compared to the RGDS modified hydrogel implanted subcutaneously (Fig. S1, ESI†). Since apoptosis requires a short time for completion (~1–2 h) only a small percentage of cells will be apoptotic at any given time in the samples. However, over a prolonged time period (*e.g.* 7 days) a large number of cells can die through this process. Our data indicate that the percentage of apoptotic cells was three times lower in the QHREDGS group (~1.5%) *versus* the RGDS group (~4.5%). The cells encapsulated in the Az-chitosan alone were not thoroughly investigated *in vivo*, since *in vitro* studies show poor cell survival at the end of cultivation (Fig. 3).

Conclusions

We demonstrated here that the QHREDGS peptide covalently bound to the non-cell adhesive Az-chitosan hydrogel promoted

attachment and viability of encapsulated cells during *in vitro* cultivation at similar levels as the RGDS peptide. Upon *in vivo* implantation, the QHREDGS peptide attenuated apoptosis better than RGDS peptide covalently bound to Az-chitosan hydrogel, yielding more healthy cardiomyocytes in implants. Further, the QHREDGS peptide promoted elongation and assembly of contractile structures. The two peptides did not differ significantly in their ability to recruit endothelial cells, however Az-chitosan-QHREDGS gel had a significantly higher percentage of SMA+ myofibroblasts compared to the Az-chitosan-RGDS hydrogel. We conclude that incorporation of the QHREDGS peptide in the soft biomaterials is a promising tool for enhancing cardiomyocyte viability and maintaining the phenotype during tissue engineering and after *in vivo* implantation.

Acknowledgements

The authors thank Ms. Jana Dengler for measurements of ET and MCR in neonatal rat heart. This work was supported by Heart and Stroke Foundation Grant-in-Aid (T6946) and NSERC Discovery Grant to M. R. A. M. is the recipient of a Canadian Institutes of Health Research (CIHR) Banting and Best Canada Graduate Scholarship.

References

- 1 C. Mathers, T. Boerma and D. Ma Fat, *Br. Med. Bull.*, 2009, **92**, 7–32.
- 2 R. Passier, L. van Laake and C. Mummery, *Nature*, 2008, **453**, 322–329.

- 3 J. Herrmann, A. Abarbanell, B. Weil, Y. Wang, M. Wang, J. Tan and D. Meldrum, *Ann. Thorac. Surg.*, 2009, **88**, 1714–1722.
- 4 S. Fazel, G. Tang, D. Angoulvant, M. Cimini, R. Weisel, R. Li and T. Yau, *Ann. Thorac. Surg.*, 2005, **79**, S2238–2247.
- 5 P. Menasche, *Semin Thorac Cardiovasc Surg.*, 2008, **20**, 131–137.
- 6 L. Gepstein, *Heart Rhythm*, 2008, **5**, S48–52.
- 7 C. Murry, L. Field and P. Menasche, *Circulation*, 2005, **112**, 3174–3183.
- 8 K. Christman and R. Lee, *J. Am. Coll. Cardiol.*, 2006, **48**, 907–913.
- 9 T. Kofidis, J. de Bruin, G. Hoyt, D. Lebl, M. Tanaka, T. Yamane, C. Chang and R. Robbins, *J. Thorac. Cardiovasc. Surg.*, 2004, **128**, 571–578.
- 10 T. Kofidis, D. Lebl, E. Martinez, G. Hoyt, M. Tanaka and R. Robbins, *Circulation*, 2005, **112**, 1173–1177.
- 11 K. Christman, A. Vardanian, Q. Fang, R. Sievers, H. Fok and R. Lee, *J. Am. Coll. Cardiol.*, 2004, **44**, 654–660.
- 12 N. Landa, L. Miller, M. Feinberg, R. Holbova, M. Shachar, I. Freeman, S. Cohen and J. Leor, *Circulation*, 2008, **117**, 1388–1396.
- 13 J. Ryu, I. Kim, S. Cho, M. Cho, K. Hwang, H. Piao, S. Piao, S. Lim, Y. Hong, C. Choi, K. Yoo and B. Kim, *Biomaterials*, 2005, **26**, 319–326.
- 14 P. Zhang, H. Zhang, H. Wang, Y. Wei and S. Hu, *Artif. Organs*, 2006, **30**, 86–93.
- 15 C. Shi, Y. Zhu, X. Ran, M. Wang, Y. Su and T. Cheng, *J. Surg. Res.*, 2006, **133**, 185–192.
- 16 I. Kim, S. Seo, H. Moon, M. Yoo, I. Park, B. Kim and C. Cho, *Biotechnol. Adv.*, 2008, **26**, 1–21.
- 17 A. Chenite, C. Chaput, D. Wang, C. Combes, M. Buschmann, C. Hoemann, J. Leroux, B. Atkinson, F. Binette and A. Selmani, *Biomaterials*, 2000, **21**, 2155–2161.
- 18 K. Ono, Y. Saito, H. Yura, K. Ishikawa, A. Kurita, T. Akaike and M. Ishihara, *J. Biomed. Mater. Res.*, 2000, **49**, 289–295.
- 19 Y. Yeo, W. Geng, T. Ito, D. Kohane, J. Burdick and M. Radisic, *J. Biomed. Mater. Res B Appl Biomater.*, 2007, **81**, 312–322.
- 20 L. Sun, M. Cui, Z. Wang, X. Feng, J. Mao, P. Chen, M. Kangtao, F. Chen and C. Zhou, *Biochem. Biophys. Res. Commun.*, 2007, **357**, 779–784.
- 21 R. Ross, *J. Card. Failure*, 2002, **8**, S326–331.
- 22 S. Dallabrida, N. Ismail, J. Oberle, B. Himes and M. Rupnick, *Circ. Res.*, 2005, **96**, e8–24.
- 23 F. Rask, S. M. Dallabrida, N. S. Ismail, Z. Amoozgar, Y. Yeo and M. Radisic, *Journal of Biomedical Materials Research Part A*, in press.
- 24 L. Bindhu and T. Abraham, *J. Appl. Polym. Sci.*, 2003, **88**, 1456–1464.
- 25 M. Graber, D. DiLillo, B. Friedman and E. Pastoriza-Munoz, *Anal. Biochem.*, 1986, **156**, 202–212.
- 26 T. Aoki, T. Ohashi, T. Matsumoto and M. Sato, *Ann. Biomed. Eng.*, 1997, **25**, 581–587.
- 27 G. C. Engelmayr Jr., M. Cheng, C. J. Bettinger, J. T. Borenstein, R. Langer and L. E. Freed, *Nat. Mater.*, 2008, **7**, 1003–1010.
- 28 D. Theret, M. Levesque, M. Sato, R. Nerem and L. Wheeler, *J. Biomech. Eng.*, 1988, **110**, 190–199.
- 29 M. Radisic, H. Park, H. Shing, T. Consi, F. Schoen, R. Langer, L. Freed and G. Vunjak-Novakovic, *Proc. Natl. Acad. Sci. U. S. A.*, 2004, **101**, 18129–18134.
- 30 R. Iyer, L. Chiu and M. Radisic, *J. Biomed. Mater. Res A*, 2009, **89**, 616–631.
- 31 S. M. Dallabrida, N. Ismail, J. R. Oberle, B. E. Himes and M. A. Rupnick, *Circ. Res.*, 2005, **96**, e8–24.
- 32 H. Fujii, Z. Sun, S. Li, J. Wu, S. Fazel, R. Weisel, H. Rakowski, J. Lindner and R. Li, *JACC: Cardiovasc. Imaging*, 2009, **2**, 869–879.
- 33 X. He, M. Chen, S. Li, S. Liu, Y. Zhong, H. McDonald Kinkaid, W. Lu, R. Weisel and R. Li, *Mol. Cell Biochem.*, 2010, **339**, 89–98.
- 34 A. Engler, C. Carag-Krieger, C. Johnson, M. Raab, H. Tang, D. Speicher, J. Sanger, J. Sanger and D. Discher, *J. Cell Sci.*, 2008, **121**, 3794–3802.
- 35 B. Bhana, R. Iyer, W. Chen, R. Zhao, K. Sider, M. Likhithpanichkul, C. Simmons and M. Radisic, *Biotechnol. Bioeng.*, 2010, **105**, 1148–1160.
- 36 J. G. Jacot, A. D. McCulloch and J. H. Omens, *Biophys. J.*, 2008, **95**, 3479–3487.
- 37 M. Ishihara, K. Obara, T. Ishizuka, M. Fujita, M. Sato, K. Masuoka, Y. Saito, H. Yura, T. Matsui, H. Hattori, M. Kikuchi and A. Kurita, *J. Biomed. Mater. Res.*, 2003, **64a**, 551–559.
- 38 J. Karp, Y. Yeo, W. Geng, C. Cannizarro, K. Yan, D. Kohane, G. Vunjak-Novakovic, R. Langer and M. Radisic, *Biomaterials*, 2006, **27**, 4755–4764.
- 39 H. Song, C. Yoon, S. Kattman, J. Dengler, S. Masse, T. Thavaratnam, M. Gewarges, K. Nanthakumar, M. Rubart, G. Keller, M. Radisic and P. Zandstra, *Proc. Natl. Acad. Sci. U. S. A.*, 2010, **107**, 3329–3334.
- 40 M. Radisic, M. Euloth, L. Yang, R. Langer, L. Freed and G. Vunjak-Novakovic, *Biotechnol. Bioeng.*, 2003, **82**, 403–414.
- 41 N. P. Brindle, P. Saharinen and K. Alitalo, *Circ. Res.*, 2006, **98**, 1014–1023.
- 42 G. Thurston, J. S. Rudge, E. Ioffe, H. Zhou, L. Ross, S. D. Croll, N. Glazer, J. Holash, D. M. McDonald and G. D. Yancopoulos, *Nat. Med.*, 2000, **6**, 460–463.
- 43 I. Kim, S. O. Moon, S. K. Park, S. W. Chae and G. Y. Koh, *Circ. Res.*, 2001, **89**, 477–479.
- 44 J. R. Gamble, J. Drew, L. Trezise, A. Underwood, M. Parsons, L. Kasminkas, J. Rudge, G. Yancopoulos and M. A. Vadas, *Circ. Res.*, 2000, **87**, 603–607.
- 45 I. Kim, J. L. Oh, Y. S. Ryu, J. N. So, W. C. Sessa, K. Walsh and G. Y. Koh, *Faseb J.*, 2002, **16**, 126–128.
- 46 Z. G. Zhang, L. Zhang, S. D. Croll and M. Chopp, *Neuroscience*, 2002, **113**, 683–687.
- 47 J. J. Tomasek, G. Gabbiani, B. Hinz, C. Chaponnier and R. A. Brown, *Nat. Rev. Mol. Cell Biol.*, 2002, **3**, 349–363.
- 48 A. Desmouliere, M. Redard, I. Darby and G. Gabbiani, *Am J Pathol*, 1995, **146**, 56–66.